European Polymer Journal 216 (2024) 113266

Contents lists available at ScienceDirect

European Polymer Journal

journal homepage: www.elsevier.com/locate/europolj

# Investigating oligo(ethylene glycol) methacrylate thermoresponsive copolymers

Fatimah [a], Pratik Gurnani [b], Gareth R. Williams [a,*]

[a] UCL School of Pharmacy, University College London, 29 – 39 Brunswick Square, London WC1N 1AX, UK
[b] Division of Molecular Therapeutics and Formulation, School of Pharmacy, University of Nottingham, Nottingham NG7 2RD, UK

A B S T R A C T

Methacrylate-based polymers are frequently used in the development of thermoresponsive smart materials for biomedical applications. Among all the routes to such polymers, reversible addition fragmentation chain transfer (RAFT) copolymerisation is one of the most widely used. This paper reports the synthesis of thermoresponsive copolymers comprising oligo(ethylene glycol) methyl ether methacrylate with Mn of 300 ($OEGMA_{300}$) and di(ethylene glycol) methyl ether methacrylate (DiEGMA). Polymers of molecular weight up to 100 kDA were obtained via RAFT polymerisation, mediated by a dithiobenzoate chain transfer agent (CTA) at 70 °C. An appropriate solvent, ratio of initiator to monomers, and minimum reaction polymerisation time were essential to provide optimum polymers. The synthesis of homogenous p($OEGMA_{300}$-co-DIEGMA) polymers with PDI of 1.1–1.2 was achieved in toluene with ≥10 h of reaction. Increasing the molecular weight of the p($OEGMA_{300}$-co-DiEGMA) polymers decreases the polydispersity index. p($OEGMA_{300}$-co-DiEGMA) polymers with Mw of 50,000 Da were successfully synthesised with lower critical solution temperatures (LCSTs) of 41.3 °C, 43.0 °C and >45 °C for $OEGMA_{300}$:DiEGMA molar ratios of 2:8, 3:7 and 4:6, respectively. Further, the LCST was not found to be affected by the polymer molecular weight. The p($OEGMA_{300}$-co-DiEGMA) polymers showed no cytotoxicity to Caco-2 cells at a concentration of 1 mg $mL^{-1}$, whereas a decrease of HDF cell viability by up to 26.5 % was seen. These polymers could be beneficial for several biomedical applications, such as developing formulations for temperature-triggered drug delivery.

## 1 Introduction

Stimuli-responsive polymers change physically and/or chemically in response to external stimuli, with examples including light, temperature, ultrasound and mechanical force [1]. Thermoresponsive polymers (TRP) are designed such that at least one of their physico-chemical properties depends on the solution temperature [2], and exhibit a phase transition temperature at which a drastic change in the solubility occurs. UCST (upper critical solution temperature) polymers are those which are insoluble at lower temperature and undergo a phase transition to become soluble upon reaching the critical temperature. Conversely, polymers in aqueous solution which become insoluble upon heating above a critical temperature are defined as exhibiting LCST (lower critical solution temperature) behaviour [1,3]. Over the past decade, the thermo-responsive properties of such polymers have been extensively studied due to their potential applications in the biomedical and drug delivery fields. Exemplar applications include nanogels [4,5], microparticles [6], tissue engineering [7]and nanoparticles [8,9].

Poly(N-isopropylacrylamide) (PNIPAM) is the most widely investigated TRP, with an LCST transition at 32 °C – relatively close to physiological temperature [10,1,11,12,13]. However, non-reacted NIPAM monomers and unwanted oligomers are found to be toxic to cells [12,14], as well as being non-biodegradable in the body [13,15,16]. There are thus some major drawbacks for biological applications. Recently, the alternative of poly(ethylene glycol methacrylate) (PEGMA) systems has attracted researchers [14,17]. PEGMAs are interesting due to their biocompatibility (both as monomers and polymer structures), as well as their resistance to the absorption of proteins [14]. PEGMA is principally constructed from poly(ethylene glycol) (PEG; up to 85 % in weight), a polymer which has been commonly used in pharmaceutical formulations and found to be non-toxic *in vitro* and *in vivo* [18,19,20]. The molecular structure of the methacrylate monomers used to construct PEGMA can be adjusted to provide a balance between hydrophobic groups (from the polymer backbone) and hydrophilic moieties (due to the ether oxygen of PEG on the branches), thus stabilising hydrogen bonds with surrounding water molecules [17,21]. Methacrylate polymers with intermediate ethylene oxide side-chains (2 ≤ ethylene oxide units < 10) exhibit LCST behaviour, with a higher LCST obtained by using longer ethylene oxide side-chains [10,17]. The thermosensitivity is thus tuneable by adjusting the ratio of the

* Corresponding author.
*E-mail address:* g.williams@ucl.ac.uk (G.R. Williams).

https://doi.org/10.1016/j.eurpolymj.2024.113266
Received 11 April 2024; Received in revised form 8 June 2024; Accepted 26 June 2024
Available online 27 June 2024

monomers that construct the polymer, as is the biodegradability. Hence, PEGMA is a promising candidate for biological applications [17].

One of the most widely used polymerisation approaches is the RAFT technique, a reversible deactivation radical polymerisation (RDRP) process that provides continuous chain growth, giving a product with low molar dispersity and high end group fidelity, and permitting access to complex polymer architectures [22]. RAFT polymerisation allows the controlled polymerisation of many monomers including (meth)acrylate, (meth)acrylamide, styrene and vinyl monomers with an appropriate choice of RAFT agent and reaction conditions [23,22,24]. However, to date there are only a few examples of methacrylate polymers of high molecular weight prepared by RAFT polymerisation. For instance, Becer et al. [10] developed an oligo(ethylene glycol) methacrylate homopolymer with Mn of 18 kDa and Constantinou et al. [25] synthesised various methacrylate block-copolymers with Mw up to 12 kDa. In other work, Emamzadeh *et al.* [8] developed thermoresponsive methacrylate block-copolymers with Mw of 31 kDa. However, libraries of high-molecular weight methacrylate copolymers beyond 60 kDa have not been reported.

The synthesises of polymers comprising $OEGMA_{300}$ and di(ethylene glycol) methyl ether methacrylate (DiEGMA) monomers have been reported previously in the literature, and their thermo-responsive behaviour is well known [26,27,8,28]. For instance, Ramírez-Jiménez et al. [29] evaluated the thermo-responsive behaviour of copolymers consisting of $OEGMA_{300}$ and DiEGMA monomers at various chain length in water and phosphate buffered saline (PBS). However, there is to date no study on how the polymerisation system affects polymer synthesis up to 100 kDa molecular weights, and how the choice of solvent and experimental conditions influences the product of such reactions. These conditions are critical in the RAFT polymerisation process [24], and thus we sought to develop more insight into them here.

The key objective of this work is to produce p(OEGMA)–co-DiEGMA copolymers from oligo(ethylene glycol) methyl ether methacrylate with Mn of 300 ($OEGMA_{300}$) and di(ethylene glycol) methyl ether methacrylate (DiEGMA) monomers by RAFT polymerisation, utilising a systematically solvent study to produce TRPs with Mw up to 100,000 Da for biomedical applications. DiEGMA and $OEGMA_{300}$ homopolymers have LCSTs of ~ 26 °C and ~ 64 °C respectively, and these species were thus chosen as monomers to construct a family of copolymers with tuneable LCST. The kinetics of the polymerisation process, and physicochemical characteristics and cytotoxicity of the resultant polymers were studied.

## 2. Materials and methods

### 2.1 Materials

Materials were sourced as follows: ethanol (Sigma-Aldrich), 1,4-dioxane (Sigma-Aldrich), hexane (Sigma-Aldrich), toluene (Sigma-Aldrich), acetonitrile (Sigma-Aldrich), 2,2,2-trifluoroethanol (TFE, Sigma-Aldrich), N,N-dimethylformamide (DMF, Sigma-Aldrich), tetrahydrofuran (THF, Sigma-Aldrich), dichloromethane (DCM, Sigma-Aldrich), 2,2′-azobis(2-methylpropionitrile) (AIBN; 98 %, Sigma-Aldrich), 4-cyano-4-(phenylcarbonothioylthio)pentanoic acid (CPPA; CTA/RAFT agent, Sigma-Aldrich), oligo(ethylene glycol) methyl ether methacrylate with Mn of 300 ($OEGMA_{300}$, Sigma-Aldrich), di(ethylene glycol) methyl ether methacrylate (DiEGMA; 98 %, Sigma-Aldrich), deuterated chloroform ($CDCl_3$, Sigma-Aldrich), Dulbecco's modified Eagle's medium containing 4500 mg/L D-glucose, L-glutamine, and 110 mg/L sodium pyruvate (DMEM-HG, Sigma-Aldrich), MEM non-essential amino acid solution (Sigma-Aldrich), penicillin (10,000 U/ml) – streptomycin (10,000 μg/ml) solution (Gibco by Life Technologies), heat inactivated fetal bovine serum (FBS, Gibco by Life Technologies), the human dermal fibroblast cell line (HDF, Life Technonologies), the colorectal carcinoma cell line Caco-2 (HTB-37, ATCC®), phosphate buffered saline tablets (PBS, VWR), 0.05 % trypsin-EDTA (Gibco by Life Technologies). All the chemicals were used as received without further purification. All the solvents used were analytical grade.

### 2.2 Copolymer synthesis

Production of a statistical copolymer was performed by RAFT polymerisation. $OEGMA_{300}$, DiEGMA, CPPA as the RAFT agent, AIBN (initiator) and a solvent were mixed in a round-bottomed flask equipped with a stirrer bar. The molar ratio of $OEGMA_{300}$:DiEGMA was varied at 2:8, 3:7 and 4:6, aiming to give a degree of polymerisation (DP) reaching targeted $M_n$ of 25,000, 50,000 and 100,000 Da. A standard procedure for laboratory scale solution polymerisation of p($OEGMA_{300}$-co-DiEGMA) copolymer was employed. Taking polymer P1 (Table 1) as a representative example, for the reaction a solution comprising $OEGMA_{300}$ (3.5 mmol), DiEGMA (14.0 mmol), AIBN ($7.1 \times 10^{-3}$ mmol), CPPA ($7.1 \times 10^{-2}$ mmol) and 4 mL of toluene was prepared in a round-bottomed flask equipped with stirrer bar. For other polymer syntheses, the amount of $OEGMA_{300}$ used was 3.5 mmol except for P3 where 7.0 mmol of $OEGMA_{300}$ was used. The solvent volume was 4.0 mL for all procedures.

In all cases, the round bottomed flask was sealed with a rubber septum and degassed with argon for ca. 20 min. Polymerisation was initiated by placing the degassed flask in an oil bath at 70 °C. Reaction was allowed to proceed for a maximum of 20 h under magnetic stirring, and then terminated by opening the polymer solution to the air and placing the flask in cool water. The separation of unreacted monomers from the polymer solution was undertaken by precipitation via drop-by-drop addition into excess hexane (20 times the polymer solution volume). Finally, the precipitated polymer was dissolved in ethanol and dried under reduced pressure.

### 2.3 Polymer characterisation

$^1$H NMR spectra of the synthesised polymers were recorded using a Bruker Ultrashield 400 MHz spectrometer. Samples of polymers were prepared by dissolving 5 mg in 0.6 mL of deuterated chloroform ($CDCl_3$). For the kinetic study, 0.2 mL of the unpurified polymer solution was added to 0.4 mL of $CDCl_3$. Two size exclusion chromatography (SEC) instruments were used to measure the number-average molecular weight ($M_n$), weight-average molecular weight ($M_w$) and polydispersity index (PDI) of the polymers. The first was equipped with a solvent pump (Viscotek VE 1121), a degasser (Viscotek VE 7510), a refractive index (RI) detector (Viscotek VE 3580) and two Styragel columns (MGHHR-M E0057 and MGHHR-M E0058). The system was calibrated with narrow molecular weight poly(methyl methacrylate) polymers as standards, and DMF used as the mobile phase. 100 μL of polymer solution in the mobile phase (40 mg $mL^{-1}$) was injected to the instrument at a rate of 1 mL $min^{-1}$ and the results presented as RI signal vs retention volume. The second instrument consisted of a Polymer Labs PL50+ gel permeation chromatography (GPC) system equipped with a differential RI detector and autosampler. This instrument used Agilent Plgel mixed-D (300 × 7.5 mm) + Plgel (5 μm) guard columns. DMF containing 0.1 % w/v lithium bromide was used as the mobile phase, with a flow rate of 1 mL $min^{-1}$ at 50 °C. Calibration was performed using polymethylmethacrylate standards (Agilent EasyVials) between 2,220,000 – 700 g/mol. Measurements were performed using 100 μL of the polymer solution in the mobile phase, giving a concentration of 2–5 mg $mL^{-1}$.

### 2.4 Determination of LCST

The synthesised polymer was dissolved in water or PBS (pH 7.4) at a concentration of 5 mg $mL^{-1}$. A volume of 200 μL of each solution was transferred into a 96-well-plate (Costar) and analysed with a temperature-controlled plate reader (Spectramax M2e, Molecular Devices) at 550 nm over the temperature range from 25 to 45 °C, with measurements taken every 1 °C. The well-plate was shaken for 1 min prior to measurement at each temperature. Six independent samples were investigated per polymer solution.

### 2.5 Physicochemical characterisation

Fourier transfer infrared (FTIR) spectra were obtained in attenuated total reflectance mode on a Perkin-Elmer Spectrum 100 instrument. Spectra were collected over the range of 4000 – 650 $cm^{-1}$ at a resolution of 1 $cm^{-1}$, with four scans collected. Differential scanning calorimetry (DSC) studies were performed on a TA instruments Q2000 calorimeter. Experiments were carried out with a temperature ramp of 10 °C $min^{-1}$ under a 50 mL $min^{-1}$ flow of nitrogen. The sample mass was 2–5 mg per measurement. For polymer analysis, the measurement was started by cooling from room temperature to −70 °C, then heating to 110 °C, and cooling again to −70 °C, all at a rate of 10 °C/min. The glass transition temperature ($T_g$) was observed from the third segment (i.e., 110 °C to −70 °C), as any solvents or impurities should have evaporated at in the previous heating run. Thermogravimetric analysis (TGA) was conducted using a Discovery instrument (TA Instruments). Each sample of 3–5 mg was heated from 40 to 600 °C at a rate of 10 °C $min^{-1}$ in an open aluminium pan. The instrument was purged with nitrogen gas at a flow of 25 mL $min^{-1}$ during analysis. The data were processed using the OriginLab software.

### 2.6 In-vitro cell toxicity

Human dermal fibroblast (HDF) cells and the colorectal adenocarcinoma cell line Caco-2 were cultured at 37 °C, under 5 % $CO_2$ in DMEM-HG supplemented with 10 % v/v heat inactivated foetal bovine serum (FBS), 1 % v/v MEM non-essential amino acids, 1 % v/v L-glutamine and 1 % v/v penicillin–streptomycin. Cells were passaged at 70–80 % confluence with 0.05 % trypsin-EDTA solution and reseeded at a concentration of $1.5 \times 10^5$ cells $mL^{-1}$. The cytotoxicity study was performed using the PrestoBlue™ viability assay, following the manufacturer instructions. The seeding density was $7.5 \times 10^4$ cells $mL^{-1}$ and $5 \times 10^4$ cells $mL^{-1}$ for HDF and Caco-2 cells, respectively. 150 μL of the harvested cells was seeded in each well of flat-bottomed 96-well-plates (Costar) and incubated for 24 h at 37 °C in a 5 % $CO_2$ environment. Solutions of the polymer in medium were filtered through a 0.22 μm filter and 30 μL of the solution was added to the each of the wells, resulting in a final polymer concentration of 1 mg $mL^{-1}$, followed by incubation for a further 24 h. Three independent experiments were performed with three replicates per plate.

## 3 Results and discussion

The RAFT polymerisation started with the reaction of $OEGMA_{300}$ and DiEGMA monomers with AIBN to form propagating radicals which further reacted with CPPA until equilibrium with the propagating radicals was reached and the reaction was terminated. After the reaction was complete, the thiocarbonylthio was found to be retained as the end group [23,30]. All the polymers synthesized were transparent violet gels, with increased viscosity noted as the polymer molecular weight increased and varied colour intensity due to the presence of the RAFT-agent as the end-group (Supporting Information, Figure S1).

### 3.1 Optimisation of polymerisation process

The choice of solvent is a crucial factor in RAFT polymerisation. A set of random $OEGMA_{300}$-co-DiEGMA co-polymers with expected $M_n$ of 50,000 was synthesized in various solvents with different polarity: toluene, 1,4-dioxane, dimethylformamide, tetrahydrofuran, and acetonitrile (Table 1). All the final polymers had a narrow polydispersity index of ca. 1.1 – 1.2 after 20 h of reaction, indicating that well-controlled polymerisation was obtained by the RAFT method (Fig. 1). Although all reactions resulted in narrow PDI, the $M_n$ of the final polymers was generally found to decrease as the dielectric constant of the solvent was increased. In toluene and 1,4-dioxane, which have dielectric constants of 2.38 and 2.21 respectively, the polymer obtained after 20 h reached > 80 % of the targeted Mn. The Mn of p($OEGMA_{300}$-co-DiEGMA) synthesised in THF (dielectric constant of 7.58) was found to be lower. When DMF or acetonitrile (dielectric constants of 36.71 and 35.94, respectively) were utilised in the polymerisation, the $M_n$ of the resultant polymers was further decreased to 35,800 and 31,300 g/mol, respectively. After 10 h of polymerisation, no further molecular weight growth was observed in all solvents, indicating that the polymerisation was complete. Based on this result, the optimum reaction time for further p($OEGMA_{300}$-co-DiEGMA) polymerisation was set at maximum of 16 h.

GPC chromatograms of the polymer prepared in toluene displayed monomodal and symmetric peaks with a clear shift to higher molecular weight over the polymerisation time (Fig. 1a). However, the polymer synthesised in 1,4-dioxane, DMF, THF and acetonitrile showed similar characteristics only over the first 6 h of polymerisation (Fig. 1b-e). After 16 h, high molar tailing was observed in the GPC chromatograms. This is attributed to the coupling of radical chain ends, thus doubling the molecular weight of the unreacted polymer chains [31], although this was not correlated with a significant change in the PDI. Further, 1,4-dioxane and THF resulted in higher PDI than the other solvents (Table 1). Similar results were obtained by Benaglia et al. [32] during the RAFT synthesis of polymethylmethacrylate (PMMA). These authors found that PMMA RAFT-polymerisation in DMF and acetonitrile was monomodal in the first 2 h and the PDI started to increase after the fourth hour of the process. Another report by Zhang et al. [33] showed that toluene was a better solvent than 1,4-dioxane for the RAFT-polymerisation of N,N-diethylacrylamide. Although the mechanism is not clear, this phenomenon could be owing to the aprotic characteristic of the solvents. In work by Pan et al. [34], the RAFT polymerisation of N-(2-hydroxypropyl) methacrylamide was negatively affected by aprotic solvents, which resulted in low conversion percentages and higher polydispersity of the polymer products. After 16 h of reaction, the monomer conversions of N-(2-hydroxypropyl) methacrylamide only reached 41 % in the aprotic solvents dimethylacetamide (DMAc), dimethylformamide (DMF) or dimethyl sulfoxide (DMSO), with the PDI of the resultant polymers lying in the range 1.29–1.40. Improved results were observed in the protic solvents methanol and water, with conversions up to 90 % and polymer PDI of 1.20–1.37.

The monomer conversion (%) was calculated by comparing the in-

**Table 1**
Results of trial p($OEGMA_{300}$-*co*-DiEGMA) RAFT polymerisation experiments in various solvents and with different molar ratios of AIBN: CPPA after 20 h of reaction.

| Trial | $OEGMA_{300}$: DiEGMA (molar ratio) | AIBN: CPPA (molar ratio) | Solvent | Dielectric constant[1] | $M_n$ (mol/g) | | PDI | Monomer conversion (%) |
|---|---|---|---|---|---|---|---|---|
| | | | | | Calculation | SEC | | |
| **1** | 2: 8 | 1: 10 | Toluene | 2.38 | 50,000 | 45,000 | 1.18 | 73.56 |
| **2** | 2: 8 | 1: 10 | 1,4-Dioxane | 2.21 | 50,000 | 41,300 | 1.21 | 73.70 |
| **3** | 2: 8 | 1: 10 | Dimethylformamide | 36.71 | 50,000 | 35,800 | 1.17 | 70.15 |
| **4** | 2: 8 | 1: 10 | Tetrahydrofuran | 7.58 | 50,000 | 39,100 | 1.20 | 74.44 |
| **5** | 2: 8 | 1: 10 | Acetonitrile | 35.94 | 50,000 | 31,300 | 1.15 | 71.42 |
| **6** | 2: 8 | 1: 20 | Toluene | 2.38 | 50,000 | – | 1.25 | – |
| **7** | 2: 8 | 1: 5 | Toluene | 2.38 | 50,000 | – | 1.84 | – |

[1] Values from [61].

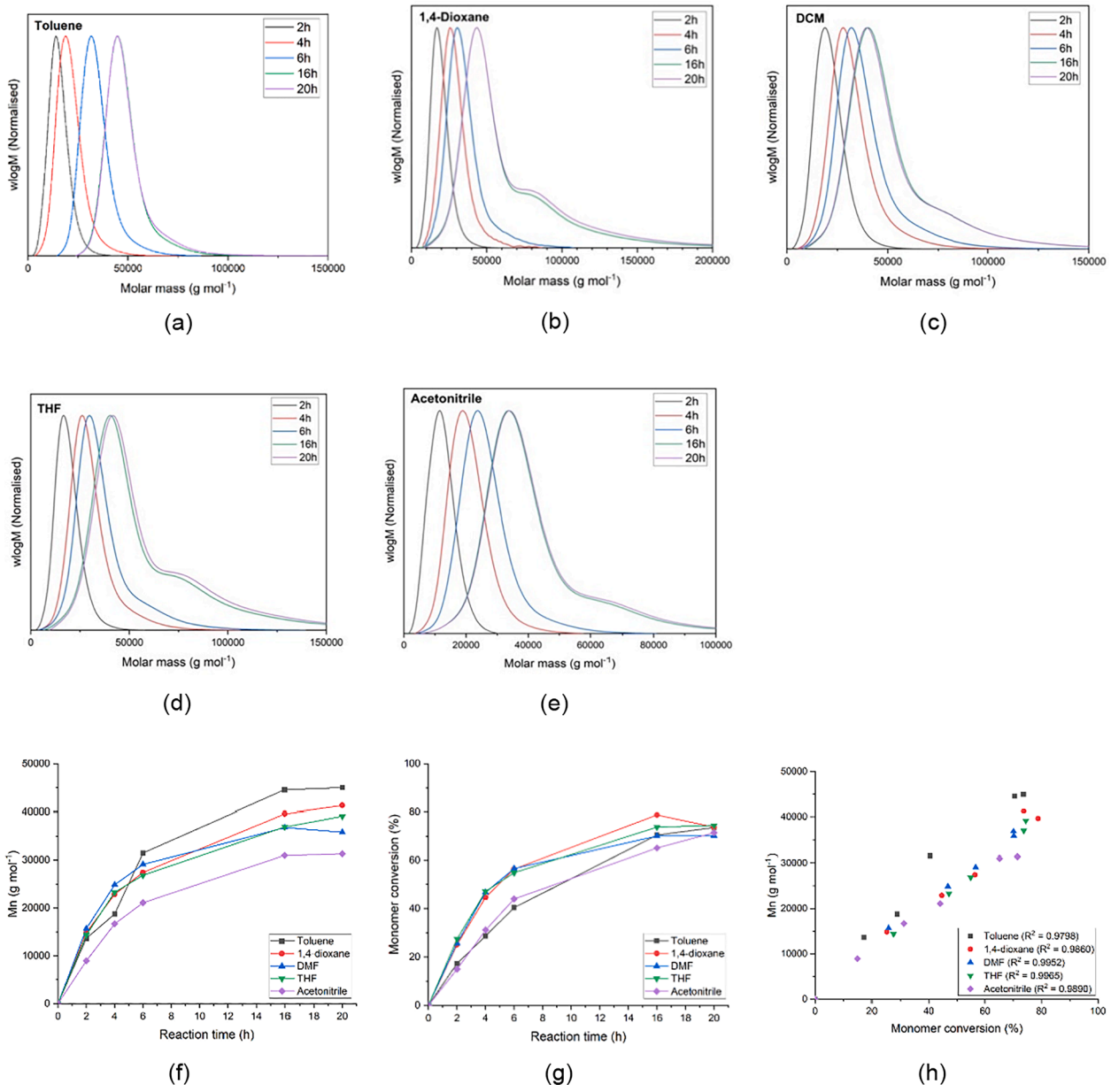


**Fig. 1.** (a) GPC traces of RAFT synthesised $OEGMA_{300}$-co-DiEGMA co-polymer in (a) toluene (Trial 1); (b) 1,4-dioxane (Trial 2); (c) DMF (Trial 3); (d) THF (Trial 4) and (e) acetonitrile (Trial 5) over 20 h of reaction; and kinetics of RAFT polymerisation of P($OEGMA_{300}$-co-DiEGMA) over 20 hours of reaction: (f) molecular weight vs time; (g) monomer conversion vs time and (h) molecular weight vs monomer conversion. (f) molecular weight vs monomer conversion ($R^2$ refers to the linear fitting coefficient for each set of data).

tegral area of the remaining unreacted monomers at $\delta = 5.34$ ppm ppm to the methyl groups of the polymer backbone at $\delta = 0.6 - 1.50$ ppm after 20 h of polymerisation, using Equation 1:

$$^1\text{H NMR monomer conversion} = \frac{^1H_p}{^1H_p + ^1H_m} \times 100 \quad (1)$$

where $^1H_p$ and $^1H_m$ represents the integral 1 proton value of the obtained polymer and the unreacted monomers, respectively. The $^1$H NMR monomer conversion calculated after 20 h is shown in Table 1. Plotting polymer conversion as a function of time for trial 1–5 shows similar results from both the NMR (Fig. 1f) and SEC data (Fig. 1g). Further, the correlation between the monomer conversion and the molecular weight remained linear during the polymerisation (Fig. 1h), confirming good control over RAFT polymerisation of $OEGMA_{300}$ and DiEGMA in all solvents used, in agreement with the literature [35].

The colour of the final products was also taken into consideration when determining the optimum solvent (Figure S1). The ratio of CPPA (the RAFT-agent at the end of polymer chain) to the monomers that constitute the polymer block determines the intensity of the colour, from dark to light violet for the shorter to the longer polymer chains. The p($OEGMA_{300}$-co-DiEGMA) polymer synthesised in toluene had a violet colour whilst the polymers synthesised in other solvents were orange in different hues. The latter observation indicated the detachment of RAFT agent from the polymer end group occurred [36], while in toluene the end group was retained. Based on these experiments, toluene was selected as the optimum solvent and 16 h as the desired reaction time.

In the trial experiments 1, 6 and 7, a series of p($OEGMA_{300}$-co-DiEGMA) copolymers with calculated $M_n$ of 50,000 Da was produced in toluene with various ratio of initiator: RAFT agent. Fig. 2 shows the GPC traces of the RAFT polymers with initiator: RAFT agent at 1:5; 1:10 and 1:20 after a reaction time of 16 h.

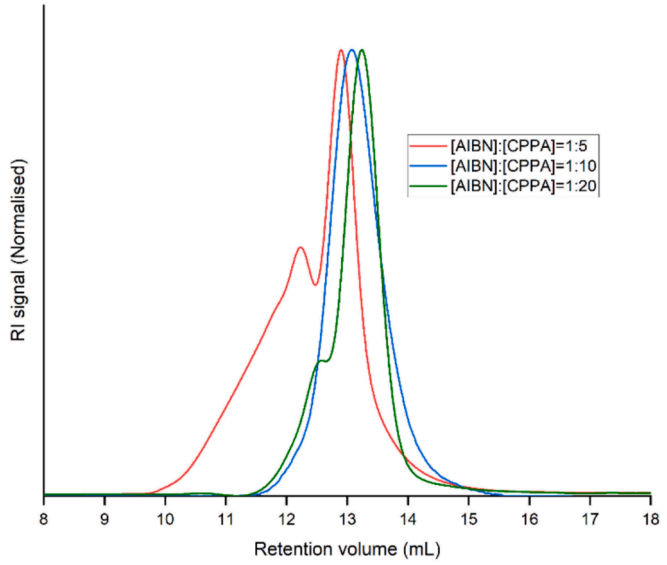


**Fig. 2.** GPC traces of polymers obtained with ratios of [AIBN]: [CPPA] = 1:20 (green curve, Trial 6); [AIBN]: [CPPA] = 1:10 (blue curve, Trial 1) and [AIBN]: [CPPA] = 1:5 (red curve, Trial 7) after 16 h of reaction in toluene. (For interpretation of the references to colour in this figure legend, the reader is referred to the web version of this article.)

The concentration of initiator could significantly affect the polymerisation process, as the number of dead chains is determined by the number of radicals generated from the initiator. Thus, reducing the concentration of AIBN initiator would lead to a minimum of "dead" polymer. However, lowering the initiator amount will also result in a longer time being required for the chains to grow as a propagating radical, and consequently a higher probability of a side reaction leading to destruction of the radical chain end. This will stop the growth of the chain and lead to the formation of dead polymer [24]. There is thus a balance between these factors, and an appropriate amount of initiator should be added.

The side reaction phenomena was seen with the polymerisation at [AIBN]: [CPPA] = 1:20, where the PDI obtained was 1.25 at a retention volume of 13.21 mL (Table 2). A small peak was observed in GPC at higher molecular weight than the main polymer population as a result of the formation of dead polymers due to prolonged reaction (Fig. 2, green line). The RAFT polymerisation rate also decreases with an increase in the RAFT agent: initiator ratio [37]. When the ratio of [AIBN]: [CPPA] was increased to 1:10, the amount of the initiator was kept low while allowing sufficient initiator concentration to provide continuous polymer growth in the system and a narrow PDI was achieved (Đ = 1.13 at retention volume of 13.09 mL; Fig. 2, blue line). Too much initiator will result in early termination and dead polymer chains [23,38]. RAFT polymerisation of $OEGMA_{300}$-co-DiEGMA with [AIBN]: [CPPA] = 1:5 resulted in two populations of polymers: the controlled polymers with RAFT agents as the end-group, and dead polymers as a consequence of AIBN over-supply in the polymerisation (Đ = 1.84 at retention volume of 12.88 mL; Fig. 2, red line). This results in a broadened distribution of molecular weights that is less controllable and contains more dead polymer chains [38]. Therefore, the ratio of [AIBN]: [CPPA] = 1:10 was optimal to use for further p($OEGMA_{300}$-co-DiEGMA) polymerisation.

**Table 2**
$M_n$, PDI and retention volume of RAFT polymers prepared in toluene with different [AIBN]: [CPPA] ratios, as determined by GPC analysis after 16 h of reaction.

| Trial | [AIBN] : [CPPA] | PDI | Retention volume (mL) | GPC shape |
|---|---|---|---|---|
| 6 | 1: 20 | 1.25 | 13.21 | Bimodal |
| 1 | 1: 10 | 1.13 | 13.09 | Monomodal |
| 7 | 1: 5 | 1.84 | 12.88 | Bimodal |

The ideal set of conditions for polymerisation thus appears to be using toluene and a 1:10 ratio of AIBN: CPPA (Trial 1). The kinetics of p($OEGMA_{300}$-co-DiEGMA) formation under these conditions were probed in more detail by NMR and SEC. Fig. 3a presents the NMR data. The peak at $\delta = 2.06$ ppm (peak (i)) before polymerisation was attributed to the methyl group of the monomers. Once the reaction has begun, the monomers are gradually converted into polymer, resulting in the disappearance of the methyl group at $\delta = 2.06$ ppm as it shifts to $\delta = 1.70$——1.00 ppm (peak (ii)) over the reaction time. Further, the C = C group of the monomers becomes saturated to form the polymer backbone, resulting in a broad peak at $\delta = 2.30$——2.00 ppm (peak (iii)).

SEC data are depicted in Fig. 3b. The RAFT method provided controlled polymerisation with monomodal molar mass distributions throughout the course of the reaction. The dispersities were all narrow, with Đ values varying from 1.14 to 1.22. The chain growth was relatively slow in the first 5 h, followed by rapid polymerisation until Mn reached the target weight.

Fig. 3c shows the calculated conversion of $OEGMA_{300}$ and DiEGMA co-polymer (determined from the $^1$H NMR plot) and the $M_n$ (from the GPC traces) over 19 h of reaction. It can be observed that the polymer growth was relatively slow in the first four hours, reaching only 20 % monomer conversion. This was probably due to the inhibition phase of the polymerisation. Upon the process reaching equilibrium, the propagation started to occur rapidly, resulting in 63 % conversion in the following four hours. Finally, as most monomers have been consumed into the polymer chain, the growth rate became slower, and termination reactions started to occur when the monomer conversion was above 70 % [38]. There is an approximately linear relationship between $M_n$ and monomer conversion (Fig. 3d).

Fig. 3e shows a plot of the natural logarithm of total monomer conversion over 19 h of reaction time which showed a pseudo-first order reaction. Some inhibition occurred during the first 4 h of the reaction, followed by rapid chain growth until most of the monomers had been consumed and then a plateau in the end of the reaction when the monomer concentration was depleted. This is the common kinetic order in RAFT polymerisation [39,40,11]. This observation shows that the radical concentration remains constant during the polymerisation and the growth of the polymer is under control [34,11,41]. Therefore, for further experiments the polymerisation was stopped after 16 h of reaction.

### 3.2 Polymer characterization

A family of p($OEGMA_{300}$-co-DiEGMA) copolymers was synthesised under the optimum conditions of [AIBN]:[CPPA] = 1:10 in toluene to obtain varied molar ratios of $OEGMA_{300}$:DiEGMA and polymer chain lengths, as detailed in Table 3. The aim here was to tune the LCST behaviour for the target application.

Fig. 4 shows the $^1$H NMR spectrum of PEGMA and DiEGMA (Fig. 4a) and p($OEGMA_{300}$-co-DiEGMA) with calculated Mn of 50,000 Da and molar ratio of $OEGMA_{300}$: DiEGMA = 2:8 (polymer P1, Fig. 4b). In the $^1$H NMR spectra of $OEGMA_{300}$ and DiEGMA monomers, twin peaks at 5.31 and 5.86 ppm are attributed to the vinyl –$CH_2$ group and the resonance at 1.69 ppm arises from the vinyl –CH group [27]. Upon coupling with other monomers to form the polymer chain, these peaks disappear as seen in Fig. 4b [42].

In the $^1$H NMR spectra of p($OEGMA_{300}$-co-DiEGMA), the $CDCl_3$ peak at 7.25 ppm was used as an internal standard [43]. The peaks around 7.60 ppm belong to the aromatic ring of the RAFT agent. These peaks are very low intensity due to the low molar ratio between the RAFT agent and the monomers that build the polymer chain. Further, the spectrum of p($OEGMA_{300}$-co-DiEGMA) reveals signals at 1.63, 1.81 and 1.90 ppm which are assigned to the saturated $CH_2$ groups on the polymer backbone. These peaks do not appear in the spectrum of the monomers,

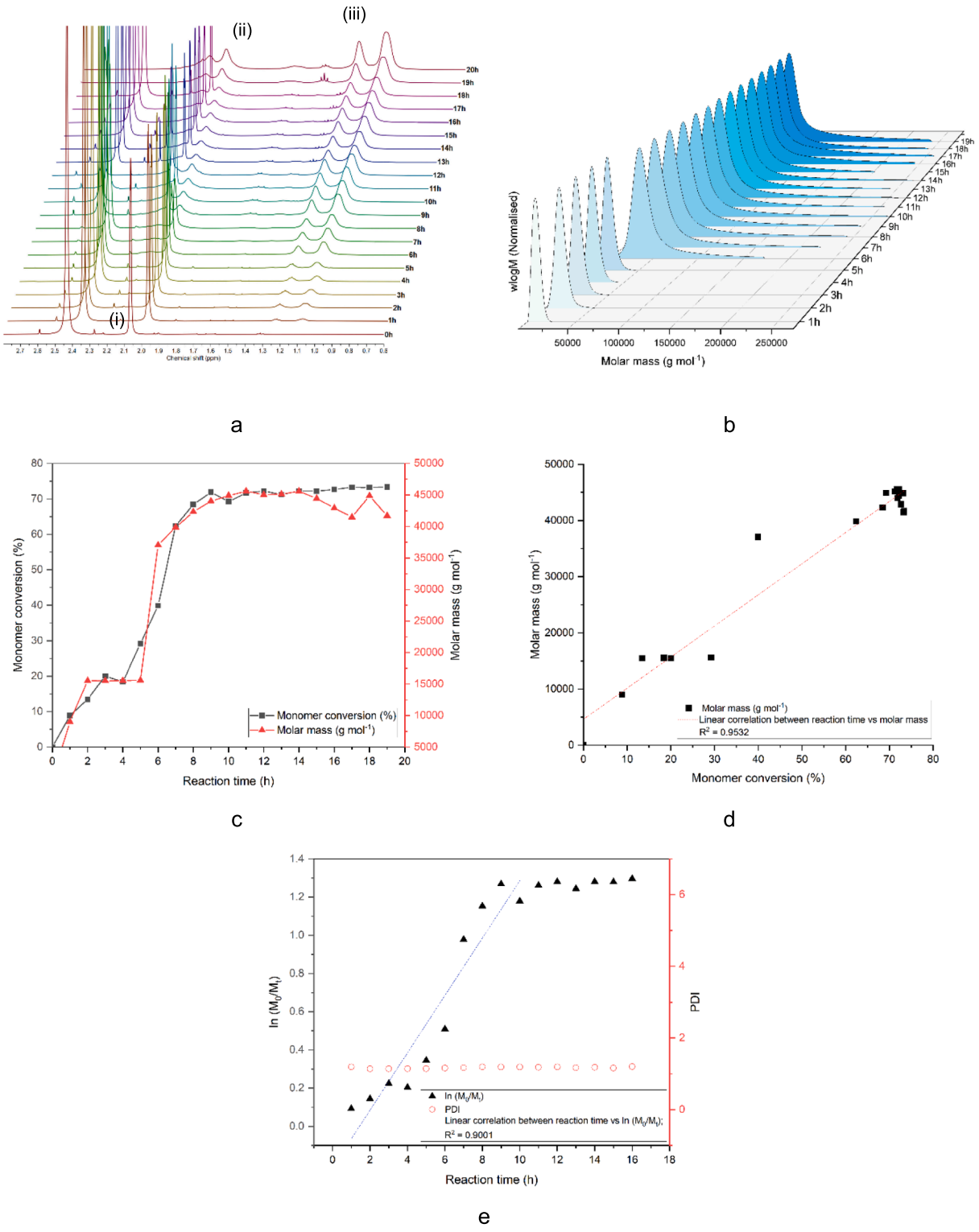


**Fig. 3.** Kinetic data from the conversion of $OEGMA_{300}$ and DiEGMA monomers into a copolymer over 20 h of reaction in Trial 1. (a) Stacked $^1H$ NMR plot ($CDCl_3$, 400 MHz). Labels refer to resonances from the (i) methyl group of monomer; (ii) methyl group of the polymer; and (iii) methylene group of polymer. (b) Overlay of recorded GPC traces. (c) Polymer growth vs time plotted as molecular weight or monomer conversion. (d) Molecular weight vs monomer conversion. (e) ln (monomer conversion) and PDI vs reaction time.

which confirmed successful polymerisation. The peaks for the methyl groups on the polymer backbone are observed at 0.88, 1.04 and 1.25, 1.42 ppm. The p($OEGMA_{300}$-co-DiEGMA) polymer architecture is knows as a brush-structure polymer, where the monomers graft to form a main backbone from the reactive group on the end of the monomers and side-chains attached to the backbone (Fig. 4b) [12]. The H atoms on the polymer brushes (side chains) gave signals at 3.55 and 3.66 ppm, while the methylene groups next to the oxygen of the ester group in the polymer side chain shows a chemical shift at 4.10 ppm. Lastly, the methyl group at the end of the polymer brushes is observed at 3.30 ppm.

**Table 3**
Properties of p(OEGMA$_{300}$-co-DiEGMA) copolymers prepared with varied chain length and molar ratio of OEGMA$_{300}$ and DiEGMA.

| Polymer | OEGMA$_{300}$: DiEGMA (molarratio) | Mn (mol/g) | | PDI |
|---|---|---|---|---|
| | | Theoretical | GPC | |
| **P1** | 2: 8 | 50,000 | 44,900 | 1.23 |
| **P2** | 3: 7 | 50,000 | 41,504 | 1.31 |
| **P3** | 4: 6 | 50,000 | 44,045 | 1.20 |
| **P4** | 2: 8 | 25,000 | 21,912 | 1.20 |
| **P5** | 2: 8 | 100,000 | 61,085 | 1.27 |

The p(OEGMA$_{300}$-co-DiEGMA) polymers P2-P5 possess similar spectra to that in Fig. 4a, and are presented in Figure S2.

The number average molecular weight (Mn) and polydispersity index (PDI) of the p(OEGMA$_{300}$-co-DiEGMA) polymer P1 – P5 were analysed by GPC using poly(methyl methacrylate) (PMMA) as the calibration standard (Fig. 4c). The final polymers were synthesised with molecular weight of 50,000 Da and in three different ratio of OEGMA$_{300}$: DiEGMA, at 2:8, 3:7 and 4:6. p(OEGMA$_{300}$:DiEGMA) polymers with ratio of OEGMA$_{300}$:DiEGMA = 2:8 were also synthesised with calculated molecular weights of 25,000 and 100,000 Da. All the syntheses resulted in narrow PDI in the range of 1.20—1.31 (Table 3). It is known that controlled polymerisation using conventional RAFT technique is achievable within the target molecular weight range of 1,000 to 100,000 Da depending on the reaction conditions [24]. In the case of P5, it seems that the targeted Mn of 100,000 Da exceeded the limit of control of RAFT polymerisation in this system. Although the PDI of P5 was narrow, the resultant molecular weight achieved was only approximately 60,000 Da (Table 3).

The IR spectra of the monomers and p(OEGMA$_{300}$-co-DiEGMA) polymer P1 (as a representative example of the polymers) are shown in Fig. 5a. The spectra of OEGMA$_{300}$ and DiEGMA show characteristic C = C stretches at 1635 cm$^{-1}$, with –CH out-of-plane olefinic bends at 937 cm$^{-1}$ and C–H in-plane bends at 1244 cm$^{-1}$. The sharp peak at 1724 cm$^{-1}$ corresponds to C = O and the alkyl ether C–O stretch is present at 1167 cm$^{-1}$ and 1104 cm$^{-1}$ [44,45]. The broad characteristic peak at 3000 – 2800 cm$^{-1}$ is attributed to the methyl –CH$_3$ stretch while the methyl –CH bend appears at 1482 – 1450 cm$^{-1}$. The bands around 1321 – 1294 cm$^{-1}$ correspond to the skeletal C–C vibrations and at 1400 – 1350 cm$^{-1}$ the methylene –CH bend can be seen. The formation of the polymer was confirmed by the disappearance of the monomer C = C stretches at 1635 cm$^{-1}$ and methylene C–H in-plane bend at 1250 cm$^{-1}$ (Fig. 5a). This finding is in agreement with other research [45]. The CPPA RAFT agent bands could not be observed by FTIR due to the very low concentration of CPPA in the polymer.

DSC traces of OEGMA$_{300}$, DiEGMA and p(OEGMA$_{300}$-co-DiEGMA) P1-P5 are depicted in Fig. 5b. The DSC curves show one glass transition temperature ($T_g$), with details summarised in Table 4. The p(OEGMA$_{300}$-co-DiEGMA) polymers showed a decrease in $T_g$ at an increased ratio of OEGMA$_{300}$ in the polymer chain P1-P3. Further, the $T_g$ value was also found to be lower with a longer polymer chain when the ratio of OEGMA$_{300}$: DiEGMA was constant, as depicted by P1, P4 and P5, which might be owing to the incorporation of OEGMA$_{300}$ which causes there to be longer side chains on the polymer. This is in agreement with research by Szabo et al. [52], which revealed that the $T_g$ value of the P(OEGMA$_{300}$) homopolymer was −56.1 °C, and P(OEGMA$_{188}$) homopolymer was −41.0 °C.

The TGA curves of the polymers are presented in Figure S3. The CPPA RAFT agent started to decompose at ca. 130 °C, which is in agreement with the literature [36]. All the polymers exhibit a small mass loss below 100 °C, corresponding to the evaporation of absorbed water and residual synthesis solvent. At temperatures between 140 °C to 270 °C, a second mass loss up to 20 % could be observed. Finally, the main polymer chain started to decompose at 300 °C, resulting in complete mass loss by ca. 400 °C. Similar TGA traces are also found in research related to the degradation of PNIPAAM-end groups [46]and methacrylate derivative-grafted polymers [47].

Poly(methyl methacrylate) (PMMA) polymers are known to decompose in two reaction steps involving terminal scission and a further random C–C scission with first onset at around 220 °C [48]. However, at longer polymer chain lengths, a lower temperature substep could be observed due to degradation initiated at the backbone chain formed during the termination reaction of the growing polymer chain [49]. To observe the decomposition characteristics of p(OEGMA$_{300}$-co-DiEGMA), DSC analysis of the polymer was conducted up to 250 °C. It can be seen that the DSC trace showed a broad and noisy endotherm at ca. 140 °C, hypothesised to be the initial degradation of the backbone (Figure S4), resulting in fragmentation of the polymer and generating small gaseous molecules such as methane and methanol [48,50].

Clear differences between the $^1$H NMR spectra before and after the decomposition phase at 250 °C were observed (Figure S5). A pair of C = C proton peaks at 5.57 and 6.13 ppm reoccurred after heating, confirming polymer chair scission and the reforming of unsaturated C = C groups. Additionally, a decreasing intensity of methyl groups at the end of the polymer brushes at 3.39 ppm and H atoms on the polymer brushes at 3.55 and 3.66 ppm were also observed after heating, confirming the shorter side chain length after decomposition [50]. Holland and Hay [51] concluded that PMMA polymer (Mw ≥ 12,900) decomposition would result from elimination of methoxycarbonyl side-chains. This could also be observed via the recurrence of H signals corresponding to the methoxycarbonyl group –COOC**H$_2$** in the decomposed side chain [51,52].

### 3.3 LCST determination

The p(OEGMA$_{300}$-co-DiEGMA) copolymer was synthesised with different ratios of OEGMA$_{300}$:DiEGMA and degrees of polymerisation to achieve a balanced copolymer with tuneable LCST. The homopolymers of OEGMA$_{300}$ and DiEGMA have LCST of ca. 64 °C and 26 °C, respectively [17]. Fig. 6 shows P1 in aqueous solution below (left) and above (right) the LCST.

Below its LCST, the copolymer in aqueous solution is fully soluble, and hence a clear and transparent solution is formed. The ether oxygens of PEG on the OEGMA$_{300}$ and DiEGMA monomers form stabilizing H-bonds with water while the backbone is hydrophobic, thus resulting in a subtle balance between hydrophilicity and hydrophobicity of the polymer in aqueous medium [17]. The equilibrium between the polymer–polymer and polymer-water interactions lies in favour of the polymer being in solution. As the temperature increases, this balance is disrupted and leads to weakened water-polymer hydrogen bonds and the polymer–polymer interactions becoming more favourable, causing the polymer to separate out from solution, becoming insoluble and giving a cloudy suspension [2,21].

Turbidimetry measurements using UV–vis spectroscopy were used to determine the LCST of p(OEGMA$_{300}$-co-DiEGMA) as presented in Table 5. Fig. 7 presents plots of transmittance as a function of temperature for the p(OEGMA$_{300}$-co-DiEGMA) polymers. The LCST of 50,000 Da p(OEGMA$_{300}$-co-DiEGMA) was determined to be 41.3 °C and 43.0 °C for P1 and P2, prepared with a molar monomer ratio of 2:8 and 3:7, respectively. The LCST of P3, with a 4:6 monomer ratio could not be quantified: the maximum temperature attainable on the measurement system is 45 °C, and at this temperature the P3 solution did not show any turbidity. It could be seen that the LCST of the polymer was strongly influenced by the OEGMA$_{300}$ and DiEGMA fractions that construct the polymer, where DiEGMA provides more hydrophilic characteristics (and thus a higher LCST) and OEGMA$_{300}$ is more hydrophobic (lowering the LCST).

Research by Lutz et al [53] and Becer et al. [10] shows that the LCST is not significantly influenced by polymer chain length, but the polymer molecular weight investigated in their work was a maximum of ~ 12,000 g/mol. Figure 7a shows that P1, P4 and P5 exhibit similar LCST

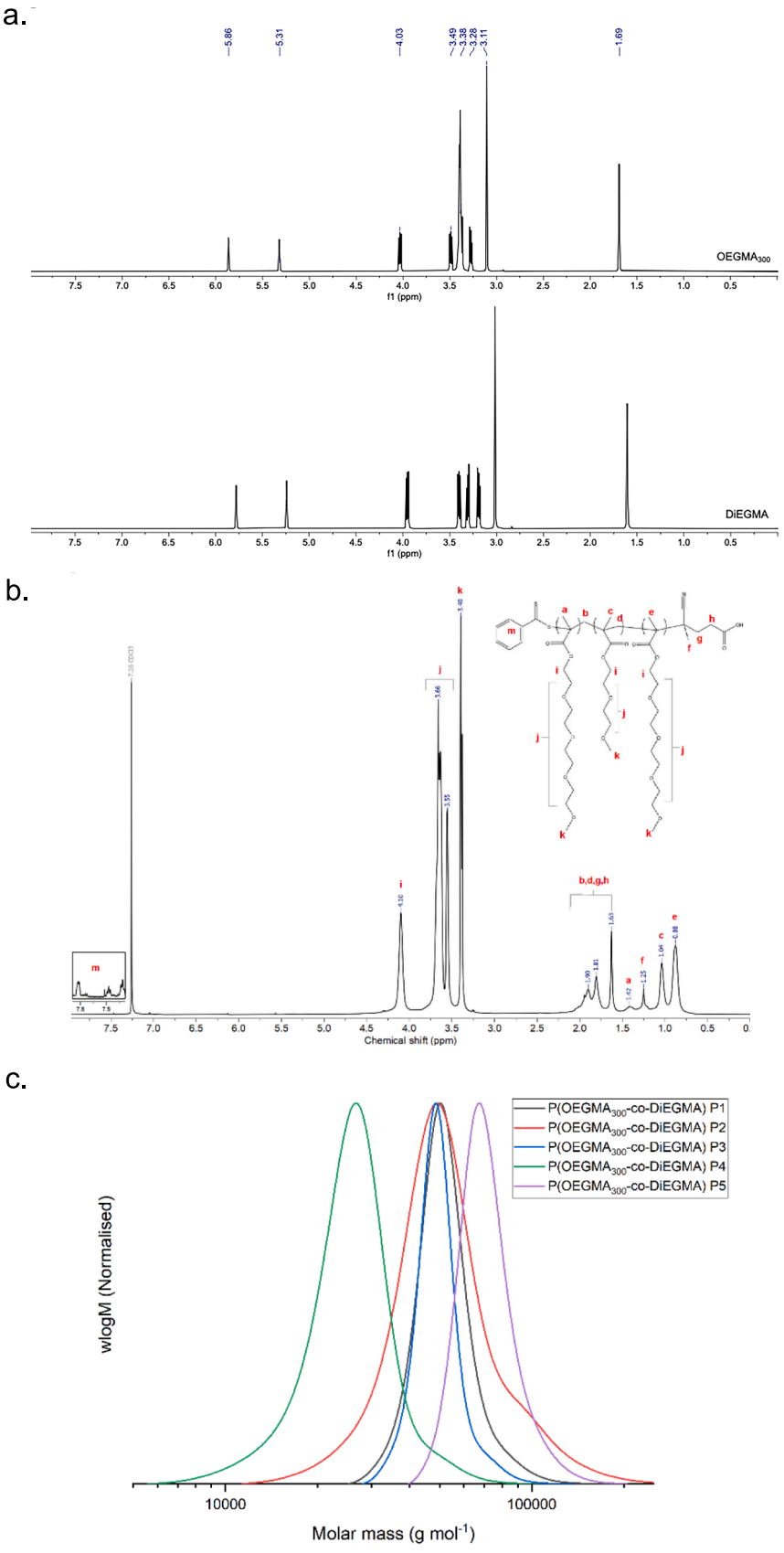


**Fig. 4.** $^{1}$H NMR spectra of (a) $OEGMA_{300}$ and DiEGMA monomers and (b) p($OEGMA_{300}$-co-DiEGMA) polymer P1 in $CDCl_3$; with (c) SEC traces of p($OEGMA_{300}$-co-DiEGMA) polymers P1 – P5.

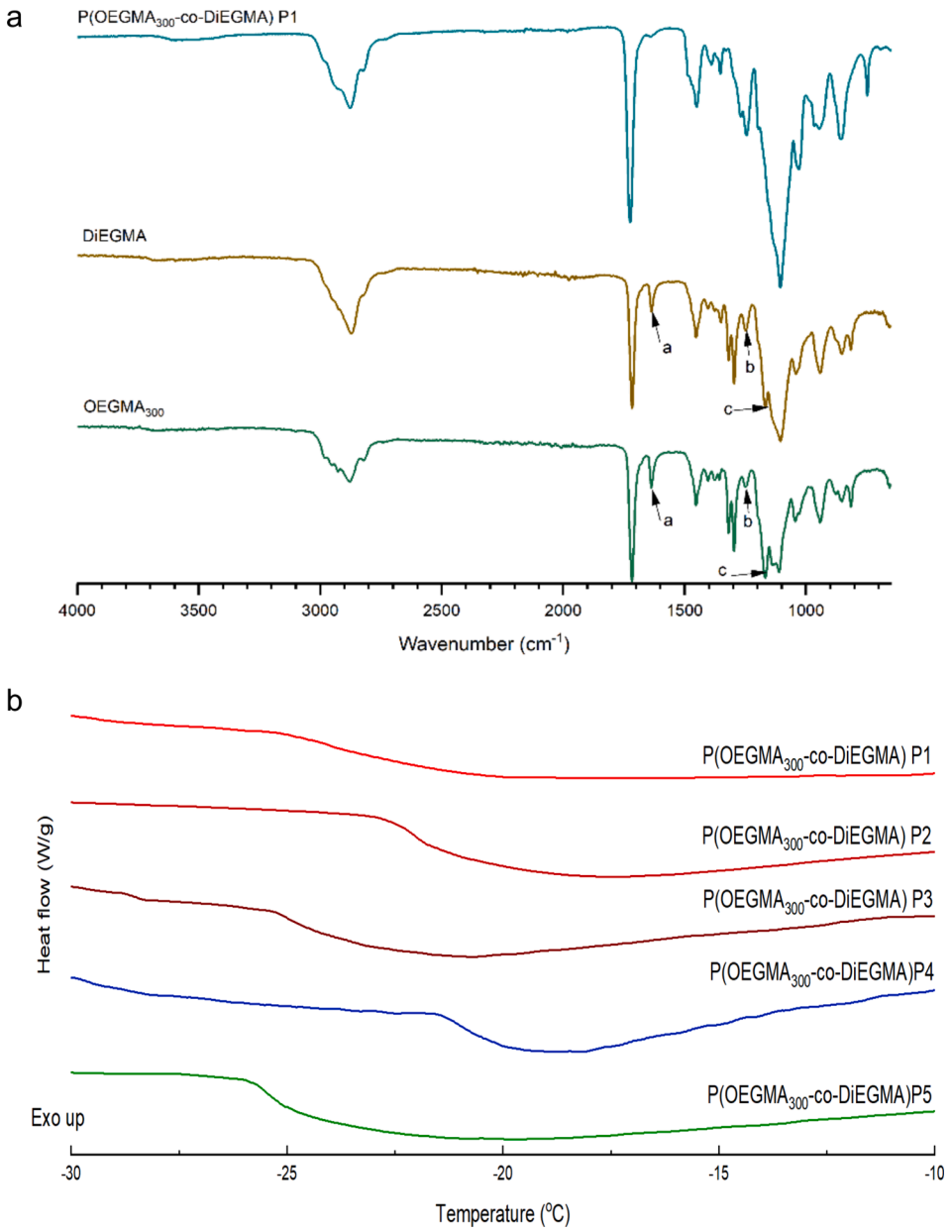


**Fig. 5.** (a) IR spectra for the monomers and P1, and (b) DSC traces (second cool) of $OEGMA_{300}$, DiEGMA and p($OEGMA_{300}$-co-DiEGMA) co-polymers P1 – P5. Key vibrational bands are marked as "a" (C=C), "b" (C-H), "c" (C=O).

**Table 4**
Glass transition temperature ($T_g$) of p($OEGMA_{300}$-co-DiEGMA) systems P1 – P5.

| Polymer | $T_g$ (°C) |
|---|---|
| P1 | −18.1 |
| P2 | −18.8 |
| P3 | −21.0 |
| P4 | −17.7 |
| P5 | −20.2 |

values at 41.3 °C, which confirms that the LCST is not significantly influenced by polymer chain length even at much higher molecular weight values.

The LCST of the polymers with $OEGMA_{300}$:DiEGMA = 2:8 was also measured in PBS at pH 7.4 (0.01 M) (Figure 7b). The LCST in PBS was 40.3 °C and 39.6 °C for P1 and P5, respectively. The LCST of the polymer in PBS is lower than in water due to the presence of salt in the buffer. The

**Fig. 6.** Photographs of P1 in aqueous solution below (left) and above (right) the LCST.

**Table 5**
LCST values of p(OEGMA$_{300}$-co-DiEGMA) P1 – P5 in water and PBS.

| Polymer in solution | LCST (°C) |
|---|---|
| P1 in water | 41.3 |
| P2 in water | 43.0 |
| P3 in water | > 45.0 |
| P4 in water | 41.3 |
| P5 in water | 41.3 |
| P1 in PBS | 40.3 |
| P5 in PBS | 39.6 |

resultant ions can interact with both the water and polymer, and hence the interactions between water and the polymer are disrupted [28,54].

### 3.4 Polymer cytotoxicity

PEG-based methacrylate derivative polymers have been reported to be non-toxic for biological applications [55,56,57]. However, the RAFT agent in the p(OEGMA$_{300}$-co-DiEGMA) polymer end group may alter its toxicity. Previous studies of the RAFT agents alone revealed a wide range of responses from non-toxic to toxic depending on the specific structure of the RAFT agents and the cell lines used [58,59]. Research conducted by Pissuwan et al. [59] showed that dithiobenzoate-ended polymers did not cause any significant toxicity over 24 h for CHO-K1, NIH3T3, and RAW264.7 cells. It was concluded that the toxicity of the RAFT polymers is not only dependant on the RAFT agent used during the synthesis, but also on the cell line used for the study as well as the functional units present in the polymer.

The toxicity of 2:8 ratio p(OEGMA$_{300}$-co-DiEGMA) with Mn 25,000 (polymer P4), 50,000 (P1) and 100,000 Da (P5) was studied on Caco2 and HDF cell lines. Fig. 8 illustrates the viability of the cells after 24 h of treatment at a concentration of 1 mg/mL. The Caco2 cell viability was 101.7 ± 24.2 %, 91.3 ± 16.9 % and 100.0 ± 9.8 % for P4, P1 and P5, respectively. In the HDF cell line, the cell viability was found to be lower, at 73.5 ± 16.6 %, 87.8 ± 21.5 % and 74.9 ± 18.0 % for P4, P1 and P5, respectively (Fig. 8). The copolymers clearly have no toxicity against the Caco-2 cells, whereas there is some toxicity to HDF cells. However, it should be noted that the polymer concentration applied was much higher than the average concentration used for common biological applications. This indicates the high cytocompatibility of the p(OEGMA$_{300}$-co-DiEGMA) polymers generated in this work. Similar results for the biocompatibility of p(DiEGMA)-based nanofibres on L929 cells have been reported previously [60].

## 4 Conclusions

A series of high-molecular weight thermoresponsive polymers comprising oligo(ethylene glycol) methyl ether methacrylate with Mn of 300 (OEGMA$_{300}$) and di(ethylene glycol) methyl ether methacrylate (DiEGMA) monomers has been successfully synthesised via the RAFT approach. The synthesis of homogenous p(OEGMA$_{300}$-co-DIEGMA) polymers with PDI of 1.1–1.2 was achieved in toluene with ≥ 10 h of reaction. p(OEGMA$_{300}$-co-DiEGMA) polymers with Mw of 50,000 Da possessed an LCST of 41.3 °C, 43.0 °C and above 45 °C for OEGMA$_{300}$:

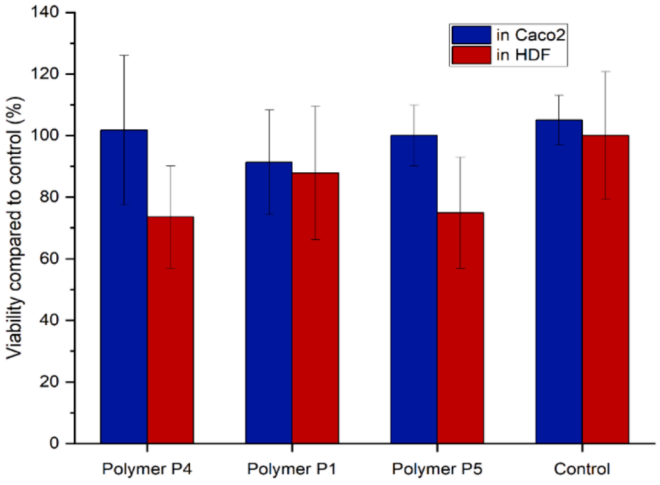


**Fig. 8.** Cytotoxicity of p(OEGMA$_{300}$-co-DiEGMA) at Mn of 25,000 (P4); 50,000 (P1) and 100,000 Da (P5) on the Caco-2 (blue) and HDF (red) cell lines at 1 mg mL$^{-1}$. Three independent experiments were performed with triplicate wells in each. (For interpretation of the references to colour in this figure legend, the reader is referred to the web version of this article.)

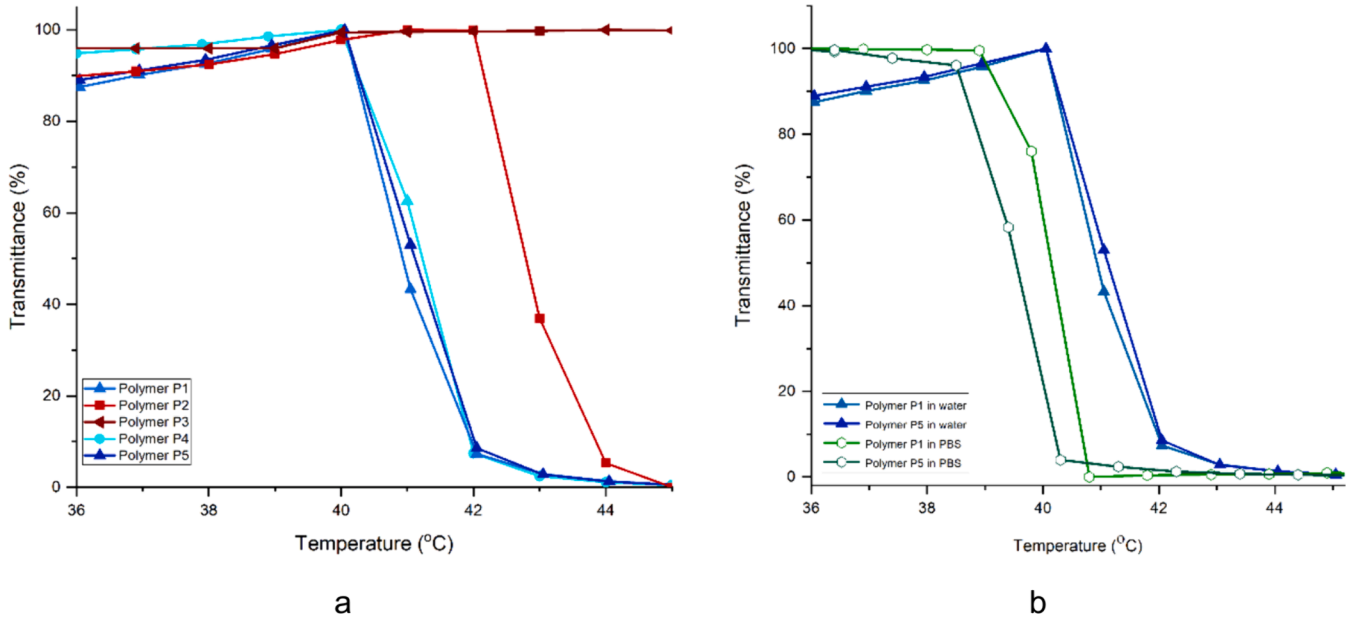


**Fig. 7.** Plot of transmittance at 550 nm as function of temperature for (a) p(OEGMA$_{300}$-co-DiEGMA) polymers P1 – P5 in deionized water; and (b) a comparison of the data for P1 and P5 in DI water and PBS.

DiEGMA monomer ratios of 2:8, 3:7 and 4:6, respectively. The molecular weight of the polymer was not found to have a marked effect on the LCST. Further, the LCST of the polymers lowered in PBS (pH 7.4) due to the presence of ionic species. In terms of toxicity, the synthesised p ($OEGMA_{300}$-co-DiEGMA) polymers showed no cytotoxicity to Caco2 cells at a concentration of 1 mg $mL^{-1}$, whereas a decrease of HDF cell viability by up to 26.5 % was seen after incubation with the polymers. These systems with targeted LCST could be beneficial for several biomedical applications, such as developing formulations form temperature-triggered drug delivery.

## CRediT authorship contribution statement

**Fatimah:** Writing – original draft, Validation, Methodology, Investigation, Funding acquisition, Formal analysis, Conceptualization. **Pratik Gurnani:** Writing – review & editing, Resources, Methodology, Formal analysis. **Gareth R. Williams:** Writing – review & editing, Validation, Supervision, Resources, Methodology, Data curation, Conceptualization.

## Declaration of competing interest

The authors declare that they have no known competing financial interests or personal relationships that could have appeared to influence the work reported in this paper.

## Data availability

Data will be made available on request.

## Acknowledgements

This research was supported by The Indonesian Endowment Fund for Education (LPDP RI) of The Ministry of Finance, The Republic of Indonesia.

## Appendix A. Supplementary data

Supplementary data to this article can be found online at https://doi.org/10.1016/j.eurpolymj.2024.113266.

## References

[1] E.S. Gil, S.M. Hudson, Stimuli-reponsive polymers and their bioconjugates, Prog. Polym. Sci. (Oxford) 29 (12) (2004) 1173–1222, https://doi.org/10.1016/j.progpolymsci.2004.08.003.
[2] A. Bordat, T. Boissenot, J. Nicolas, N. Tsapis, Thermoresponsive polymer nanocarriers for biomedical applications, Adv. Drug Deliv. Rev. 138 (2019) 167–192, https://doi.org/10.1016/j.addr.2018.10.005.
[3] M. Sponchioni, U. Capasso Palmiero, D. Moscatelli, Thermo-responsive polymers: Applications of smart materials in drug delivery and tissue engineering, Mater. Sci. Eng. C 102 (April) (2019) 589–605, https://doi.org/10.1016/j.msec.2019.04.069.
[4] B. Aktan, L. Chambre, R. Sanyal, A. Sanyal, "Clickable" nanogels via thermally driven self-assembly of polymers: facile access to targeted imaging platforms using thiol – maleimide conjugation, 2017. Doi: 10.1021/acs.biomac.6b01576.
[5] I. Altinbasak, S. Kocak, R. Sanyal, A. Sanyal, Redox-responsive nanogels for drug-delivery: thiol–maleimide and thiol–disulfide exchange chemistry as orthogonal tools for fabrication and degradation, Polym. Chem. 14 (34) (2023) 3897–3905, https://doi.org/10.1039/d3py00210a.
[6] J. Bai, Y. Zhang, L. Chen, H. Yan, C. Zhang, L. Liu, X. Xu, Synthesis and characterization of paclitaxel-imprinted microparticles for controlled release of an anticancer drug, Mater. Sci. Eng. C 92 (September 2017) (2018) 338–348, https://doi.org/10.1016/j.msec.2018.06.062.
[7] R.E. Young, J. Graf, I. Miserocchi, R.M. Van Horn, M.B. Gordon, C.R. Anderson, L. S. Sefcik, Optimizing the alignment of thermoresponsive poly(N-isopropyl acrylamide) electrospun nanofibers for tissue engineering applications: A factorial design of experiments approach, PLoS One 14 (7) (2019) 1–15, https://doi.org/10.1371/journal.pone.0219254.
[8] M. Emamzadeh, D. Desmaële, P. Couvreur, G. Pasparakis, Dual controlled delivery of squalenoyl-gemcitabine and paclitaxel using thermo-responsive polymeric micelles for pancreatic cancer, J. Mater. Chem. B 6 (15) (2018) 2230–2239, https://doi.org/10.1039/c7tb02899g.
[9] G. Yilmaz, B. Demir, S. Timur, C.R. Becer, Poly(methacrylic acid)-coated gold nanoparticles: functional platforms for theranostic applications, 2016. Doi: 10.1021/acs.biomac.6b00706.
[10] C.R. Becer, S. Hahn, M.W.M. Fijten, H.M.L. Thijs, R. Hoogenboom, U.S. Schubert, Libraries of methacrylic acid and oligo (ethylene glycol) methacrylate copolymers with LCST behavior, J. Polym. Sci. A Polym. Chem. (2008) 7138–7147, 10.1002/pola.
[11] A.E. Smith, X. Xu, C.L. Mccormick, Stimuli-responsive amphiphilic (co) polymers via RAFT polymerization, Prog. Polym. Sci. 35 (2010) 45–93, https://doi.org/10.1016/j.progpolymsci.2009.11.005.
[12] G. Conzatti, S. Cavalie, C. Combes, J. Torrisani, N. Carrere, A. Tourrette, PNIPAM grafted surfaces through ATRP and RAFT polymerization: Chemistry and bioadhesion, Colloids Surf. B Biointerfaces 151 (2017) 143–155, https://doi.org/10.1016/j.colsurfb.2016.12.007.
[13] E. Dalgakiran, H. Tatlipinar, A Computational study on the LCST phase transition of a POEGMA type thermoresponsive block copolymer: effect of water ordering and individual behavior of blocks, J. Phys. Chem. B 123 (6) (2019) 1283–1293, https://doi.org/10.1021/acs.jpcb.8b11775.
[14] Q. Li, A.P. Constantinou, T.K. Georgiou, A library of thermoresponsive PEG-based methacrylate homopolymers: How do the molar mass and number of ethylene glycol groups affect the cloud point? J. Polym. Sci. 59 (3) (2020) 230–239, https://doi.org/10.1002/pol.20200720.
[15] M. Karimi, A. Ghasemi, P. Sahandi Zangabad, R. Rahighi, S.M. Moosavi Basri, H. Mirshekari, et al., Smart micro/nanoparticles in stimulus-responsive drug/gene delivery systems. Chemical Society Reviews, Roy. Soc. Chem. 45 (2016), https://doi.org/10.1039/C5CS00798D.
[16] A. Mellati, M. Valizadeh Kiamahalleh, S. Dai, J. Bi, B. Jin, H. Zhang, Influence of polymer molecular weight on the in vitro cytotoxicity of poly (N-isopropylacrylamide), Mater. Sci. Eng. C 59 (2016) 509–513, https://doi.org/10.1016/j.msec.2015.10.043.
[17] J.F. Lutz, Polymerization of oligo(ethylene glycol) (meth)acrylates: Toward new generations of smart biocompatible materials, J. Polym. Sci. A Polym. Chem. 46 (11) (2008) 3459–3470, https://doi.org/10.1002/pola.22706.
[18] J.L. Fang, M.M. Vanlandingham, F.A. Beland, R.P. Felton, M.P. Maisha, G.R. Olson, et al., Toxicity of high-molecular-weight polyethylene glycols in Sprague Dawley rats, Toxicol. Lett. 359 (January) (2022) 22–30, https://doi.org/10.1016/j.toxlet.2022.01.011.
[19] L. Kobylinska, I. Patereha, N. Finiuk, N. Mitina, A. Riabtseva, I. Kotsyumbas, et al., Comb-like PEG-containing polymeric composition as low toxic drug nanocarrier, Cancer Nanotechnol. 9 (1) (2018), https://doi.org/10.1186/s12645-018-0045-5.
[20] H.P. Le Khanh, D. Nemes, Á. Rusznyák, Z. Ujhelyi, P. Fehér, F. Fenyvesi, et al., Comparative investigation of cellular effects of polyethylene glycol (PEG) derivatives, Polymers 14 (2) (2022) 1–15, https://doi.org/10.3390/polym14020279.
[21] J.F. Lutz, K. Weichenhan, O. Akdemir, A. Hoth, About the phase transitions in aqueous solutions of thermoresponsive copolymers and hydrogels based on 2- (2-methoxyethoxy) ethyl methacrylate and oligo (ethylene glycol) methacrylate, Macromolecules 40 (2007) 2503–2508.
[22] G. Moad, RAFT polymerization to form stimuli-responsive polymers, Polym. Chem. 8 (1) (2017) 177–219, https://doi.org/10.1039/c6py01849a.
[23] A. Gregory, M.H. Stenzel, Complex polymer architectures via RAFT polymerization: From fundamental process to extending the scope using click chemistry and nature's building blocks, Prog. Polym. Sci. (Oxford) 37 (1) (2012) 38–105, https://doi.org/10.1016/j.progpolymsci.2011.08.004.
[24] S. Perrier, 50th anniversary perspective: RAFT polymerization - a user guide, Macromolecules 50 (19) (2017) 7433–7447, https://doi.org/10.1021/acs.macromol.7b00767.
[25] A.P. Constantinou, B. Zhan, T.K. Georgiou, Tuning the gelation of thermoresponsive gels based on triblock terpolymers, Macromolecules 54 (4) (2021) 1943–1960, https://doi.org/10.1021/acs.macromol.0c02533.
[26] C. Cheng, A.J. Convertine, P.S. Stayton, J.D. Bryers, Multifunctional triblock copolymers for intracellular messenger RNA delivery, Biomaterials 33 (28) (2012) 6868–6876, https://doi.org/10.1016/j.biomaterials.2012.06.020.
[27] I. Emaldi, S. Hamzehlou, J. Sanchez-Dolado, J.R. Leiza, Kinetics of the aqueous-phase copolymerization of MAA and PEGMA macromonomer: Influence of monomer concentration and side chain length of PEGMA, Processes 5 (2) (2017), https://doi.org/10.3390/pr5020019.
[28] Y.Y. Khine, Y. Jiang, A. Dag, H. Lu, M.H. Stenzel, Dual-responsive pH and temperature sensitive nanoparticles based on methacrylic acid and di(ethylene glycol) methyl ether methacrylate for the triggered release of drugs, Macromol. Biosci. 15 (8) (2015) 1091–1104, https://doi.org/10.1002/mabi.201500057.
[29] A. Ramírez-Jiménez, K.A. Montoya-villegas, A. Licea-claverie, M.A. Gónzalez-Ayón, A. Ram, K.A. Montoya-villegas, et al., Tunable thermo-responsive copolymers from DEGMA and OEGMA synthesized by RAFT polymerization and the effect of the concentration and saline phosphate buffer on its phase transition, Polymers 11 (10) (2019), https://doi.org/10.3390/polym11101657.
[30] G. Moad, E. Rizzardo, S.H. Thang, Living radical polymerization by the RAFT process, Aust. J. Chem. 58 (2005), https://doi.org/10.1071/CH05072.
[31] Y. Zheng, Y. Huang, B.C. Benicewicz, A useful method for preparing mixed brush polymer grafted nanoparticles by polymerizing block copolymers from surfaces with reversed monomer addition sequence, Macromol. Rapid Commun. 38 (19) (2017) 1–6, https://doi.org/10.1002/marc.201700300.
[32] M. Benaglia, E. Rizzardo, A. Alberti, M. Guerra, Searching for more effective agents and conditions for the RAFT polymerization of MMA: Influence of dithioester substituents, solvent, and temperature, Macromolecules 38 (8) (2005) 3129–3140, https://doi.org/10.1021/ma0480650.

[33] X. Zhang, O. Giani, S. Monge, J. Robin, RAFT polymerization of N, N-diethylacrylamide: Influence of chain transfer agent and solvent on kinetics and induction period, Polymer 51 (14) (2010) 2947–2953, https://doi.org/10.1016/j.polymer.2010.04.073.
[34] X. Pan, F. Zhang, B. Choi, Y. Luo, X. Guo, A. Feng, Effect of solvents on the RAFT polymerization of N- (2-hydroxypropyl) methacrylamide, Eur. Polym. J. 115 (2019) 166–172, https://doi.org/10.1016/j.eurpolymj.2019.03.016.
[35] B. Luan, B.W. Muir, J. Zhu, X. Hao, A RAFT copolymerization of NIPAM and HPMA and evaluation of thermo-responsive properties of poly(NIPAM-co-HPMA), RSC Adv. 6 (92) (2016) 89925–89933, https://doi.org/10.1039/c6ra22722h.
[36] H. Willcock, R.K. O'Reilly, End group removal and modification of RAFT polymers, Polym. Chem. 1 (2) (2010) 149–157, https://doi.org/10.1039/b9py00340a.
[37] F. Huo, X. Wang, Y. Zhang, X. Zhang, J. Xu, W. Zhang, RAFT dispersion polymerization of styrene in water/alcohol: The solvent effect on polymer particle growth during polymer chain propagation, Macromol. Chem. Phys. 214 (8) (2013) 902–911, https://doi.org/10.1002/macp.201200640.
[38] P. Vana, T.P. Davis, C. Barner-Kowollik, Kinetic analysis of reversible addition fragmentation chain transfer (RAFT) polymerizations: Conditions for inhibition, retardation, and optimum living polymerization, Macromol. Theory Simul. 11 (8) (2002) 823–835, https://doi.org/10.1002/1521-3919(20021101)11:8<823::AID-MATS823>3.0.CO;2-R.
[39] O. Colombani, A.O. Messiaen, P. Castignolles, Polymerization kinetics: monitoring monomer conversion using an internal standard and the key role of sample t (2011) *88*(1).
[40] Y. Qu, F. Huo, Q. Li, X. He, S. Li, W. Zhang, Polymer Chemistry terpolymer nano-objects by seeded RAFT, Polym. Chem. 5 (2014) 5569–5577, https://doi.org/10.1039/C4PY00510D.
[41] S.I. Yusa, Y. Konishi, Y. Mitsukami, T. Yamamoto, Y. Morishima, pH-responsive micellization of amine-containing cationic diblock copolymers prepared by reversible addition-fragmentation chain transfer (RAFT) radical polymerization, Polym. J. 37 (7) (2005) 480–488, https://doi.org/10.1295/polymj.37.480.
[42] H. Hussain, K.Y. Mya, C. He, Self-assembly of brush-like poly[poly(ethylene glycol) methyl ether methacrylate] synthesized via aqueous atom transfer radical polymerization, Langmuir 24 (23) (2008) 13279–13286, https://doi.org/10.1021/la802734e.
[43] G.R. Fulmer, A. Miller, N. Sherden, H. Gottlieb, A. Nudelman, B. Stoltz, et al., NMR chemical shifts of common laboratory solvents as trace impurities, Organometallics 29 (2010) 2176–2179, https://doi.org/10.1021/jo971176v.
[44] S.Y. Chan, W.S. Choo, D.J. Young, X.J. Loh, Thixotropic supramolecular pectin-poly(ethylene glycol) methacrylate (PEGMA) hydrogels, Polymers 8 (11) (2016) 1–12, https://doi.org/10.3390/polym8110404.
[45] F. Hu, K.G. Neoh, L. Cen, E.T. Kang, Cellular response to magnetic nanoparticles "PEGylated" via surface-initiated atom transfer radical polymerization, Biomacromolecules 7 (3) (2006) 809–816, https://doi.org/10.1021/bm050870e.
[46] K. Bauri, S.G. Roy, S. Arora, R.K. Dey, A. Goswami, G. Madras, P. De, Thermal degradation kinetics of thermoresponsive poly(N- isopropylacrylamide-co-N, N-dimethylacrylamide) copolymers prepared via RAFT polymerization, J. Therm. Anal. Calorim. 111 (1) (2013) 753–761, https://doi.org/10.1007/s10973-012-2344-0.
[47] A. Ramírez-Jiménez, C. Alvarez-Lorenzo, A. Concheiro, E. Bucio, Temperature-responsiveness and biocompatibility of DEGMA/OEGMA radiation-grafted onto PP and LDPE films, Radiat. Phys. Chem. 99 (2014) 53–61, https://doi.org/10.1016/j.radphyschem.2014.02.013.
[48] U. Ali, K.J.B.A. Karim, N.A. Buang, A review of the properties and applications of poly (methyl methacrylate) (PMMA), Polym. Rev. 55 (4) (2015) 678–705, https://doi.org/10.1080/15583724.2015.1031377.
[49] J.D. Peterson, S. Vyazovkin, C.A. Wight, Stabilizing effect of oxygen on thermal degradation of poly(methyl methacrylate), Macromol. Rapid Commun. 20 (9) (1999) 480–483, https://doi.org/10.1002/(sici)1521-3927(19990901)20:9<480::aid-marc480>3.3.co;2-z.
[50] W.R. Zeng, S.F. Li, W.K. Chow, Review on chemical reactions of burning poly (methyl methacrylate) PMMA, J. Fire Sci. 20 (5) (2002) 401–433, https://doi.org/10.1177/0734904102020005482.
[51] B.J. Holland, J.N. Hay, The kinetics and mechanisms of the thermal degradation of poly(methyl methacrylate) studied by thermal analysis-Fourier transform infrared spectroscopy, Polymer 42 (11) (2001) 4825–4835, https://doi.org/10.1016/S0032-3861(00)00923-X.
[52] Á. Szabó, G. Szarka, B. Iván, Synthesis of poly(poly(ethylene glycol) methacrylate)-polyisobutylene ABA block copolymers by the combination of quasiliving carbocationic and atom transfer radical polymerizations, Macromol. Rapid Commun. 36 (2) (2015) 238–248, https://doi.org/10.1002/marc.201400469.
[53] J.F. Lutz, Ö. Akdemir, A. Hoth, Point by point comparison of two thermosensitive polymers exhibiting a similar LCST: Is the age of poly(NIPAM) over? J. Am. Chem. Soc. 128 (40) (2006) 13046–13047, https://doi.org/10.1021/ja065324n.
[54] Y. Zhang, P.S. Cremer, Interactions between macromolecules and ions: the Hofmeister series, Curr. Opin. Chem. Biol. 10 (6) (2006) 658–663, https://doi.org/10.1016/j.cbpa.2006.09.020.
[55] J.F. Lutz, J. Andrieu, S. Üzgün, C. Rudolph, S. Agarwal, Biocompatible, thermoresponsive, and biodegradable: Simple preparation of "All-in-one" biorelevant polymers, Macromolecules 40 (24) (2007) 8540–8543, https://doi.org/10.1021/ma7021474.
[56] Z. Qu, H. Xu, H. Gu, Synthesis and biomedical applications of poly((meth)acrylic acid) brushes, ACS Appl. Mater. Interfaces 7 (27) (2015) 14537–14551, https://doi.org/10.1021/acsami.5b02912.
[57] M. Ulasan, E. Yavuz, E.U. Bagriacik, Y. Cengeloglu, M.S. Yavuz, Biocompatible thermoresponsive PEGMA nanoparticles crosslinked with cleavable disulfide-based crosslinker for dual drug release, J. Biomed. Mater. Res. - Part A 103 (1) (2015) 243–251, https://doi.org/10.1002/jbm.a.35146.
[58] A. Gregory, M.H. Stenzel, The use of reversible addition fragmentation chain transfer polymerization for drug delivery systems, Expert Opin. Drug Deliv. 8 (2) (2011) 237–269, https://doi.org/10.1517/17425247.2011.548381.
[59] D. Pissuwan, C. Boyer, K. Gunasekaran, T.P. Davis, V. Bulmus, In vitro cytotoxicity of RAFT polymers, Biomacromolecules 11 (2) (2010) 412–420, https://doi.org/10.1021/bm901129x.
[60] H. Li, G.R. Williams, J. Wu, Y. Lv, X. Sun, H. Wu, L.M. Zhu, Thermosensitive nanofibers loaded with ciprofloxacin as antibacterial wound dressing materials, Int. J. Pharm. 517 (1–2) (2017) 135–147, https://doi.org/10.1016/j.ijpharm.2016.12.008.
[61] C. Reichardt, T. Welton, Solvents and Solvent Effects in Organic Chemistry, WILEY-VCH Verlag GmbH & Co. KGaA, Weinheim, 2011.